

# Design of Spatially Varying Orientation Lattice Structures Using Triply Periodic Minimal Surfaces

Chongyi Wei, Douglas E Smith\*

Department of Mechanical Engineering, Baylor University, Waco, TX 76706

## Abstract

Interest continues to grow for lattice structures produced by additive manufacturing methods that are described by triply periodic minimal surface (TPMS). Tunable parameters that define the TPMS provide unique design flexibility where prior research has focused on designing hybrid or functionally graded TPMS structures. In this paper, a new strategy is proposed to include an orientation angle and volume fraction of each lattice cell simultaneously when defining structures derived from TPMS. The algorithm iteratively solves an underlying partial differential equation with the finite difference method to obtain a smooth, continuous lattice structure with a spatially varying orientation angle. The resulting lattice structure can be combined with other types of TPMS models using Gaussian radial basis and distance functions to achieve multi-TPMS lattice designs. The spatially varying lattice structures can also take the advantage of the directional effective modulus of TPMS to improve the strength the performance of lattice design.

## 1. Introduction

The mechanical and structural compatibility between orthopedic implant and human body is vital for successful implantation since a large mismatch in modulus can lead to stress shielding due to the uneven stress distribution at the bone-implant interface [1], [2]. Cellular lattice structures have been shown to be ideal for tailoring the properties of implants so as to avoid stress shielding. Within the wide range of lattice structures often considered, triply periodic minimal surface (TPMS) structures offer a unique combination of strength and biological compatibility [3]. The advancement in additive manufacturing has greatly facilitated the fabrication of lattices and thus allowed for the adaptation in the design process in biomaterials. Therefore, lattice structures are increasingly employed in numerous applications, such as tissue engineering and other areas of mechanical engineering [4-6].

Yoo [7] developed an efficient internal pore architecture design system based on a triply periodic minimal surface unit cell library and associated computational methods to assemble TPMS unit cells into an entire scaffold model. Due to the unique design flexibility of TPMS lattice structures, the lattice material properties can be easily tuned to produce a desired output property. When the unit cell porosity (defined as  $1 - \rho$ ) and/or the unit cell size within a lattice is spatially varied to achieve a desired functionality, it is referred as functional grading [8]. In addition, a hybrid lattice structure can be obtained by combining two or more type of lattice structures together [9]. Further, the implicit surface mathematical function of TPMS lattice offers great advantage for modifying the cellular topology to generate anisotropic properties. However, there are limitations when tailoring the spatial structure and its properties when employing a

single type of TPMS lattice. For example, as evident from the mathematic function, only one iso-surface parameter can be tuned to change the relative density.

A variety of heterogeneous porous scaffold with gradients in porosity and pore size has been designed by using an efficient implicit interpolation method [10]. Numerical results show that the proposed scaffold design method has the potential benefits for accurately controlling the spatial porosity distribution within an arbitrarily shaped scaffold while maintaining the advantage of the TPMS-based unit cell. Afshar et al. [11] performed experimental and numerical investigations to determine the mechanical properties and deformation mechanisms of a linearly graded porosity scaffold. His work showed that the energy absorption for a uniform lattice is higher than those for graded structures and depends on loading direction. It is possible not only to change porosity through TPMS-based lattice structures, but pore architecture can be spatially varied to combine mechanical responses of different pore architecture.

Cheikho et al. [12] presented an advanced and versatile method to design graded circular porous 2D structures based on the conformal mapping of unit cells. His approach provided porous lattices obtained using a periodic transformation into a circular pattern by controlling the phase and amplitude of the periodic domain. The versatility allowed for tunable anisotropy by selecting the most appropriate structure for a given clinical application, depending on the desired porosity, pore size, and effective mechanical properties. Ma [13] proposed a design approach for heterogeneous porous scaffolds, which was obtained by discretizing the original model using the conformal refinement of the hexahedral mesh followed by a mapping of the TPMS unit onto existing mesh elements with shape functions. The TPMS lattice generated on the uniform grid was mapped into the predefined mesh patterns such that the re-meshed scaffold could be designed to the appropriate elastic properties.

To the best of our best knowledge, there is no studies that discuss TPMS lattice structures with both spatial varying infill volume fraction and orientation. Consequently, the first objective of the current study is to present an advanced framework for designing spatially varying TPMS lattices by changing the relative density and orientation for each unit lattice cell. Secondly, the design of heterogeneous lattice with spatially varying properties is demonstrated by two hybridization methods with irregular boundaries. Lastly, the versatility and limitations of the proposed method and its potential application to various tissue applications is discussed.

## **2. Methodology**

### **2.1. The design of spatially varying TPMS lattice**

TPMS lattice structures [14] are typically defined mathematically to have an approximately zero mean curvature at every point on the surface without self-intersection. A widely used TPMS form is the Schwarz's Primitive-surface [15] as appearing in Fig. 1 (a), where the minimal surface is defined by the level set function

$$F(x, y, z) = \cos(ax) + \cos(ay) + \cos(az) - t > 0 \quad (1)$$

where the parameter  $t$  controls the continuity of the cell surface which determines the volumetric solid bounded by the surface, and  $a$  defines the size of cubic unit cell. When  $F(x, y, z) = 0$ , it

defines a 3D boundary between positive  $F$  and negative  $F$ . Specifically, a candidate structure can be modeled using a 3D surface given by  $F(x, y, z) - t = 0$  which defines a wide range of unit cell lattices with different volume fractions defined by  $t$ . Otherwise, the  $F(x, y, z)$  can be modified to define other types of TPMS lattice structure, such as Gyroid and IWP shown as Fig. 1 (b) and (c) (not studied here).

The level set function in Eq. (1) is limited to being able to the generation of uniform TPMS structures which only require the size of the unit cell size and the parameter  $t$ . The uniform TPMS has been extended to include a continuous sigmoid weight function to form hybrid types of TPMS structures with a functional dependance on the coordinate location [9]. These hybrid structure have a unit cell orientation that remains unchanged. In addition, other research has shown that 3D periodic structures can be modeled by the interference to a four non-coplanar laser beams in the photonic crystals of physics field [16]. Here it is desirable to functionally grade and/or spatially vary the periodicity of the structure to form a metamaterial. The initial approach to develop a spatially varying lattice was adopted to guide the flow of the light in a preferred direction in prior work [17].

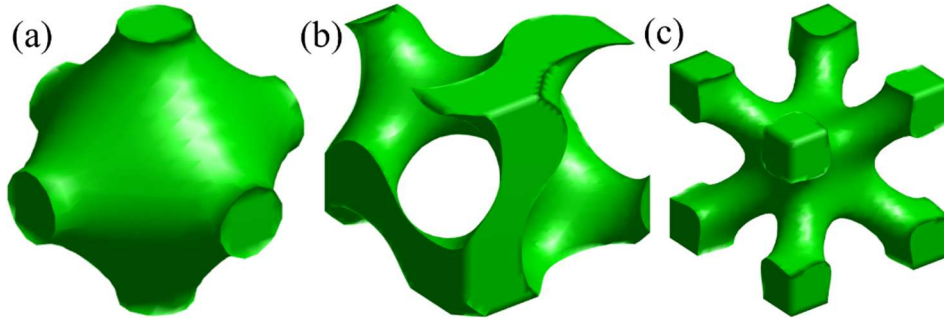


Fig. 1 TPMS unit cell: (a) Primitive type unit cell; (b) Gyroid type unit cell; (c) IWP type unit cell. The shown TPMS structure with relative density 0.3, the  $t$  value is 0.7066, 0.6044 and 0.0049 respectively.

To define a spatially orientation varying TPMS, the basic unit cell defined in Eq. (1) which describes a specific geometry is spatially varied to the form the final hybrid lattice. To this end, a periodic unit cell can be decomposed into a complex Fourier series where each term is spatially harmonic which can be interpreted as a one-dimensional sinusoidal grating that are combined to reconstruct the original unit cell. A finite set of spatial harmonics is truncated to construct the unit cell for practical implementation as

$$\varepsilon_{uc}(\vec{s}) = \sum_{i=1}^M \alpha_i e^{j\vec{K}_i \vec{s}} \quad (2)$$

where  $\alpha_i$  represents the Fourier coefficient of the  $i^{th}$  spatial harmonic, obtained from the decomposition of the baseline unit cell. Otherwise, the specific expression can be reformulated as a generalized one as Eq. (2). In the above equation,  $\vec{s}$  is position, and  $\vec{K}_i$  is the grating vector associated with the  $i^{th}$  spatial harmonics can be calculated by Eq. (2)

$$\vec{K}_i = K_x \hat{x} + K_y \hat{y} + K_z \hat{z} \quad (3)$$

where the magnitude of  $\vec{K}_i$  is defined as

$$\vec{K} = \frac{2\pi}{\Lambda} \quad (4)$$

where  $\Lambda$  is the period of grating. Alternatively, the Primitive type of TPMS lattice is defined by small set of spatial harmonics [18] where the grating vector is the linear combination of the reciprocal vector of the lattice. The formulation of the Primitive type of lattice grating vector is defined in a manner similar to Eq. (1) as

$$\begin{aligned} \vec{K}_1 &= \frac{2\pi}{\Lambda} \hat{x} \\ \vec{K}_2 &= \frac{2\pi}{\Lambda} \hat{y} \\ \vec{K}_3 &= \frac{2\pi}{\Lambda} \hat{z} \end{aligned} \quad (5)$$

where  $(\hat{x}, \hat{y}, \hat{z})$  is the coordinate position. In this form the unit cell orientation and infill volume fraction must be defined as a function of position which requires that the vector  $\vec{K}$  become a function of position to spatially vary the grating. Orientation variation in the x-y plane of  $\vec{K}$  can be computed using the rotation matrix

$$R_z(\theta) = \begin{bmatrix} \cos(\theta) & -\sin(\theta) & 0 \\ \sin(\theta) & \cos(\theta) & 0 \\ 0 & 0 & 1 \end{bmatrix} \quad (6)$$

As the vector  $\vec{K}$  becomes  $\vec{K}(\vec{s})$ , it is tempting to calculate the  $i_{th}$  spatial harmonic according to Eq. (2). However, this approach fails to construct the desired grating when the vector  $\vec{K}$  is a function of position.

$$\varepsilon_i(\vec{s}) \neq \alpha_i e^{j\vec{K}_i(\vec{s}) \cdot \vec{s}} \quad (7)$$

In order to incorporate the arbitrary spatial orientation variance in the grating, an intermediate function  $\Phi(\vec{s})$  called the grating phase (or the mapping function) is introduced. The grating phase is related to the grating vector by the gradient operation as

$$\nabla\Phi(\vec{s}) = \vec{K}(\vec{s}) \quad (8)$$

The grating phase is introduced to minimize the potential distortion of the final spatially variant lattice [20]. It is necessary to solve Eq. (8) numerically to determine the grating phase. Since there is no analytical solution for Eq. (8), it may be solved by the central finite differential method iteratively with incorporated the boundary equations [21]

$$\Phi_x = \begin{cases} \Phi_{o|2,j,k} - \frac{\Delta x}{2} (K_{x|2,j,k} + K_{x|1,j,k}) & \text{for } i = 1 \\ \frac{\Phi_{o|i-1,j,k} + \Phi_{o|i+1,j,k}}{2} - \frac{\Delta x}{4} (K_{x|i-1,j,k} + K_{x|i+1,j,k}) & 2 < i < N_x - 1 \\ \Phi_{o|N_x-1,j,k} - \frac{\Delta x}{2} (K_{x|N_x,j,k} + K_{x|N_x-1,j,k}) & \text{for } i = N_x \end{cases} \quad (9)$$

$$\Phi_{y|i,j,k} = \begin{cases} \Phi_{o|i,2,k} - \frac{\Delta y}{2} (K_{y|i,2,k} + K_{y|i,1,k}) & \text{for } j = 1 \\ \frac{\Phi_{o|i,j-1,k} + \Phi_{o|i,j+1,k}}{2} - \frac{\Delta y}{4} (K_{y|i,j-1,k} + K_{y|i,j+1,k}) & 2 < j < N_y - 1 \\ \Phi_{o|i,N_y-1,k} - \frac{\Delta y}{4} (K_{y|i,N_y,k} + K_{y|i,N_y-1,k}) & \text{for } j = N_y \end{cases} \quad (10)$$

$$\Phi_{z|i,j,k} = \begin{cases} \Phi_{o|i,j,2} - \frac{\Delta z}{2} (K_{z|i,j,2} + K_{z|i,j,1}) & \text{for } k = 1 \\ \frac{\Phi_{o|i,j,k-1} + \Phi_{o|i,j,k+1}}{2} - \frac{\Delta z}{4} (K_{z|i,j,k-1} + K_{z|i,j,k+1}) & 2 < k < N_z - 1 \\ \Phi_{o|i,j,N_z-1} - \frac{\Delta z}{2} (K_{z|N_z,j,k} + K_{z|i,j,N_z-1}) & \text{for } k = N_z \end{cases} \quad (11)$$

The terms  $K_{x|i,j,k}$ ,  $K_{y|i,j,k}$ , and  $K_{z|i,j,k}$  are the matrices containing the components of  $K$  across the grid after the orientation included using the rotation matrix in Eq. (8). The iterative grating phase is calculated as

$$\Phi_{new} = \frac{\Phi_x + \Phi_y + \Phi_z}{3} \quad (12)$$

To simplify the implementation of the algorithm, the function describing grating phase  $\Phi$  is initialized to zero. After numerically computing a solution to Eq. (8), the spatially varying lattice can be reevaluated with incorporating the mapping function  $\Phi(\vec{s})$  into the exponential expression

$$\varepsilon_v(\vec{s}) = \alpha_m e^{i\Phi(\vec{s})} \quad (13)$$

The imaginary part of above equation is ignored, and a preliminary spatially varying lattice is constructed by summation of 1D spatial grating and extraction of the real part

$$\varepsilon(\vec{s}) = Re \left[ \sum_{i=1}^M \varepsilon_v(\vec{s}) \right] \quad (14)$$

For the other periodic unit cell in 2D or 3D, the generalization from the planar grating above to spatial variant lattice is straightforward. The single unit cell that describes the periodic structure that is to be spatially varied needs to be transformed into a set of planar gratings by Fourier transform, and the periodic array of elements are reduced into a Discrete Fourier Transform (DFT) which is then truncated to limit the number of terms. Therefore, the DFT is performed on the baseline unit cell to obtain each planar grating. Each of these resulting gratings are then spatially varied individually by including the orientation and accumulated to obtain the overall final lattice.

The spatially varying cell volume fraction over the lattice is incorporated following the solution of the gradient equation governing the orientation as described above. There are two methods for mapping the relative volume fraction to the complete lattice structure. The first one is based on average density where the difference in relative density between adjacent cells is averaged has been shown lead to smooth geometric transition [22]. Secondly, the spatially variant fill fraction of the TPMS lattice structure can be implemented by a threshold technique to the preliminary binary distribution given as

$$\varepsilon(\vec{s}) = \begin{cases} \varepsilon_1, & \varepsilon'(\vec{s}) < \gamma(\vec{s}) \\ \varepsilon_2, & \varepsilon'(\vec{s}) \geq \gamma(\vec{s}) \end{cases} \quad (15)$$

where  $\gamma(\vec{s})$  is the interpolated value from the previous calculation of the single unit cell relative volume fraction obtained by varying the iso-surface parameter  $t$  [17]. After the unit lattice cell are established from the threshold method, a linear interpolation is utilized to construct the relative density for the complete lattice structure.

## **2.2 Designing heterogeneous TPMS lattice structure**

The natural structure has specific porous structures in different regions according to the service requirements, which leads to the heterogeneous structures [23]. Considering a simple geometrical transition function, the heterogeneous TPMS lattice structure can be constructed by a weighted summation defined by sigmoid function [9]

$$F = \sum_{i=1}^n w_i \cdot F_i(x) \geq 0 \quad (16)$$

where  $F_i$  is the level set function for the substructure, and the weight functions  $w_i$  are defined by

$$w_i(x) = \frac{e^{(-k_i(G(x,y,z))^2)}}{\sum_{j=1}^n e^{(-k_j(G(x,y,z))^2)}} \quad (17)$$

where  $G(x, y, z)$  defines the transition boundary of the heterogeneous lattice, and  $k_j$  is parameter that controls the width of the transition boundary.

### **2.2.1. Heterogeneous TPMS design by Gaussian radial basic function**

If the desired model comprises an irregular transition shape, there is no continuous function to define the intersection region. The Gaussian Radial Basic Function (GRBF) may be used to construct a unique function from given control points [24] to provide a more robust means to capture the transition. Implementing the GRBF requires the solving of a set of linear functions for the  $\beta_i$  as

$$\begin{bmatrix} \Omega(1,1) & \cdots & \Omega(1,m) \\ \vdots & \ddots & \vdots \\ \Omega(m,1) & \cdots & \Omega(m,m) \end{bmatrix} \begin{bmatrix} \beta_1 \\ \vdots \\ \beta_m \end{bmatrix} = \begin{bmatrix} 1 \\ \vdots \\ 1 \end{bmatrix} \quad (18)$$

where

$$\Omega(i,j) = e^{\left(-\frac{(x-x_i)^2}{\delta^2}\right)} \quad (19)$$

and the weight function is defined by

$$\alpha(X) = \sum_{i=1}^m \beta_i e^{\left(-\frac{(x-x_i)^2}{\delta^2}\right)} \quad (20)$$

Once the control line segment is represented by the Gaussian Radial Basic Function, the heterogeneous hybrid structure is constructed by the weight function of Eq. (16).

### **2.2.2. Distance field of a control line segment**

In order to represent the line segment with basic function explicitly, the distance function was introduced to accommodate the poly shape of the transition boundary for heterogeneous TPMS structures. The distance field [25] can represent a piecewise of control points which can be defined by

$$\mathbf{d}_i(\mathbf{x}) = \|\mathbf{x} - \mathbf{x}_i\| \quad (21)$$

A control line segment of two points can be defined by

$$\mathbf{x} = \mathbf{x}_1 + (\mathbf{x}_2 - \mathbf{x}_1)t \quad (22)$$

For different  $t$ , Eq. (22) represents the line segments in the  $\mathbf{x}$  coordinate space. Therefore, the distance field  $\mathbf{d}(\mathbf{x})$  of the line segments can be defined in a piecewise manner as

$$d(\mathbf{x}) = \begin{cases} \|\mathbf{x} - \mathbf{x}_1\|, & t < 0 \\ \|\mathbf{x} - \mathbf{x}_t\|, & 0 \leq t \leq 1 \\ \|\mathbf{x} - \mathbf{x}_2\|, & t \geq 1 \end{cases} \quad (23)$$

where  $t$  and  $\mathbf{x}_t$  are determined by,

$$\begin{cases} (\mathbf{x}_t - \mathbf{x}) \cdot (\mathbf{x}_2 - \mathbf{x}_1) = 0 \\ \mathbf{x}_t = \mathbf{x}_1 + (\mathbf{x}_2 - \mathbf{x}_1)t \end{cases} \quad (24)$$

Eq. (23) can be approximated by a continuous function which yields a structurally smooth result as

$$d(\mathbf{x}) = \frac{\|\mathbf{x} - \mathbf{x}_1\|}{1 + e^{k_d t}} + \frac{\|\mathbf{x} - \mathbf{x}_t\|}{(1 + e^{-k_d t})(1 + e^{k_d(t-1)})} + \frac{\|\mathbf{x} - \mathbf{x}_2\|}{1 + e^{k_d(1-t)}} \quad (25)$$

where  $k_d$  is a parameter for controlling the transition gradients between adjacent regions for  $t$ . Based on the distance field function, the irregular control line segments can be represented by a

continuous function, which could be incorporated in to the TPMS surface function by sigmoid weight function.

### **3. Methods Implementation and Results**

#### **3.1. Spatially varying TPMS lattice structure**

As an example of constructing of spatially varying orientation TPMS lattice structure, the orientation distribution and relative density distribution field need to be defined firstly. The varying angle distribution can be generated by some mathematic function or the optimized results from topology optimization. After solving Eq. (7) numerically with Eq. (8), the grating phase  $\Phi$  can be incorporated into the exponential functions to further construct the 3D surface for TPMS lattice. The predefined orientation distribution and reconstructed spatially varying TPMS for gradually varying and self-defined varying field appear in Fig.2 and Fig.3 respectively.

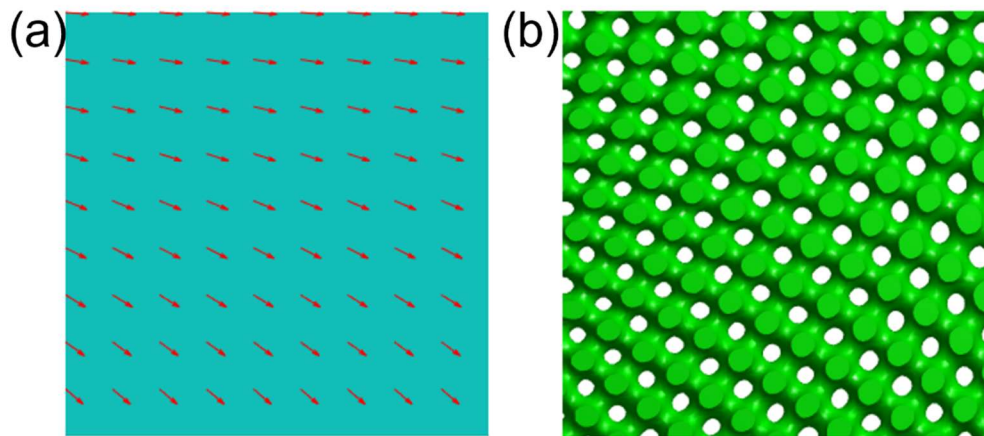


Fig. 2 The uniform gradual spatially varying Primitive TPMS lattice: (a) the varying lattice orientation and relative density distribution; (b) the reconstructed TPMS lattice.

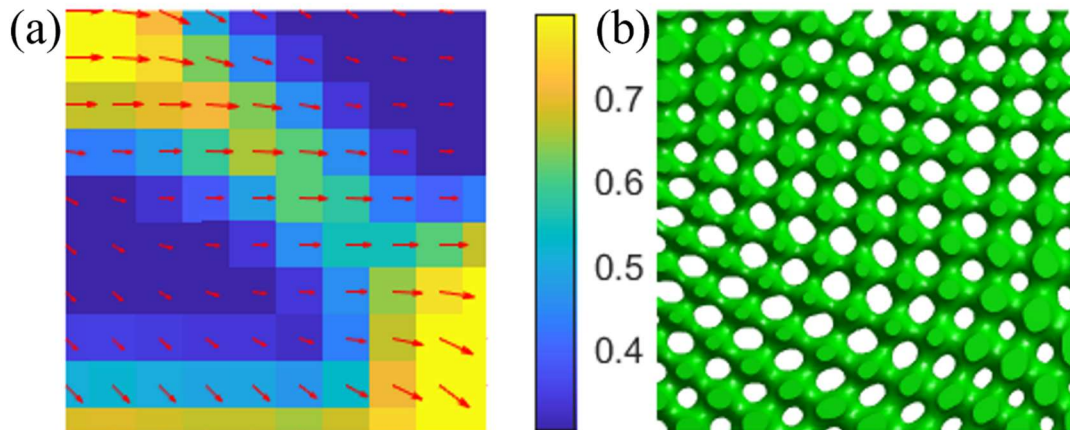


Fig. 3 The self-defined spatially varying Primitive TPMS lattice: (a) the varying lattice orientation and relative density distribution; (b) the reconstructed TPMS lattice.

### **3.2. Laminate or recursive TPMS lattice design**

Yang [26] proposed a skewed TPMS lattice with a coordinate transformation to tune the anisotropy for a single TPMS cell rather than combining various TPMS types with weight coefficients. Yang's skew transformation can be viewed as a shift in the global coordinate of the cubic cell for TPMS lattice, the relationship is defined as

$$F_1(x', y, z) > 0, \text{ where } x' = x - (z + 1) \tan \alpha_{xz} \quad (26)$$

where  $\alpha_{xz}$  is the angle for the skew transformation,  $F_1$  is skewed 3D iso-surface.

In addition, a hybrid TPMS lattice with varying layer orientation can be generated by combining a skewed TPMS lattice structure with a continuous sigmoid function as in Eq. (16), and the laminate (a concept borrowed from composite structure) lattice structure can be obtained by using the sigmoid function recursively shown as Fig. 4 (a). However, this method may lead to the structural discontinuity between two layers. The spatially varying lattice algorithm proposed in the current research can also be utilized to generate the laminate lattice with predefined orientation filed but better microstructure transition shown as Fig. 4 (b).

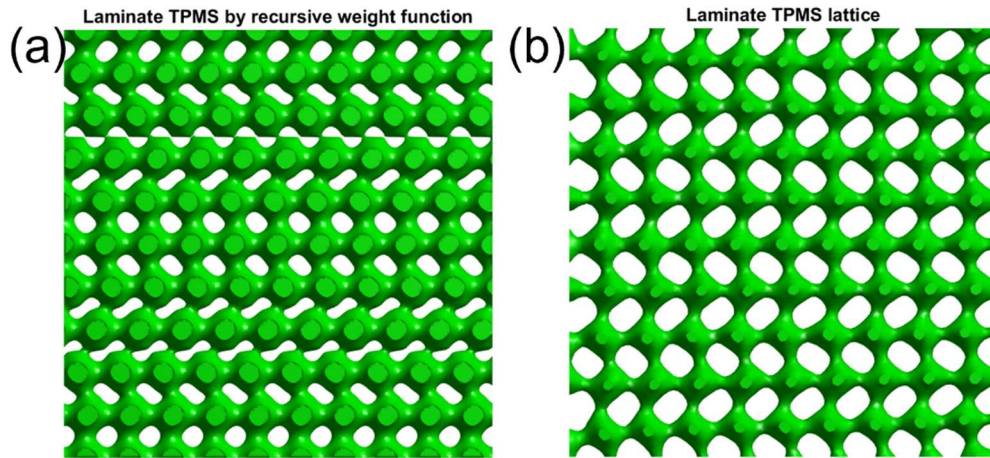


Fig. 4 The laminate TPMS designed: (a) the laminate TPMS generated by hybrid with skew transformation; (b) the laminate TPMS generated by spatial varying transformation.

### **3.3. Hybrid heterogeneous TPMS lattice**

A hybrid TPMS lattice can also be constructed using a weight function based on the sigmoid function in Eq. (16) where the hybrid transition area comes from the location function defined in Eq. (17).

Since GRBF is a real-valued function that depends on the distance between the input and some fixed points, the sum of radial function can be used to approximate the given boundary. An example of a computed heterogeneous TPMS with variant orientation for Primitive structures generated by GRBF appears in Fig. 5, where a uniform Gyroid and IWP lattice is also included that both have an irregular enclosed shape. Unfortunately, the lattice orientation leads to noncontinuous structure and defects on the transition boundary. Therefore, the GRBF method needs to be refined to apply on spatially orientation varying TPMS lattice structures.

Alternatively, complex line segments given by control points are represented by the distance function in Eq. (25) are introduced. Here the distance function is incorporated into the sigmoid weight function to tune the transition area between different lattice types. The heterogeneous lattice with variant orientation angles for the Primitive type lattice is shown as Fig. 6 where the distance field function shows a good hybrid TPMS lattice structure compared to Gaussian Radian Basic Function representation.

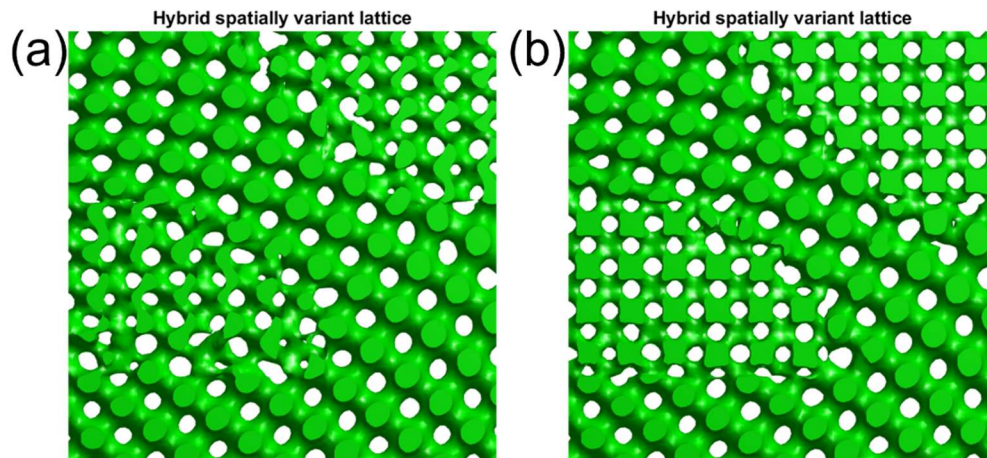


Fig. 5 Heterogeneous TPMS generated by GRBF: (a) the combination of P type and Gyroid type TPMS; (b) the combination of P type and IWP type TPMS.

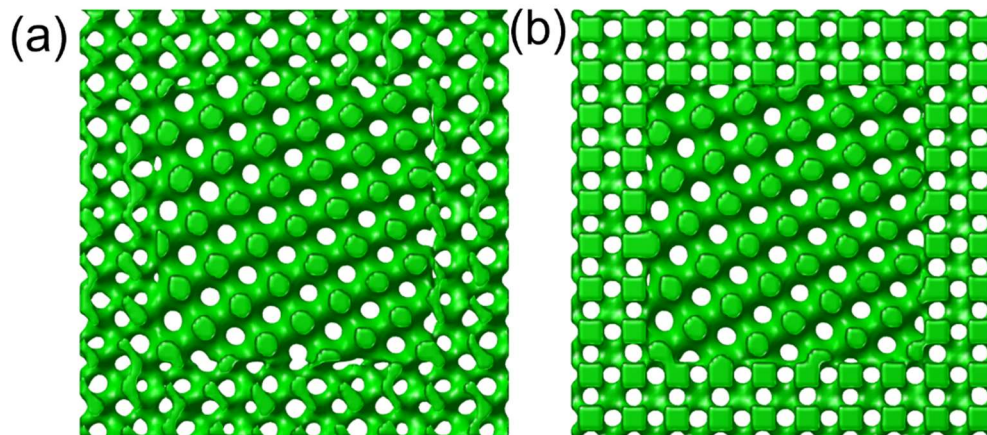


Fig. 6 Heterogeneous TPMS generated by distance field function: (a) the combination of P type and Gyroid type TPMS; (b) the combination of P type and IWP type TPMS.

#### **4. Discussion and limitation**

The spatial varying algorithm provides a significant advantage for accommodating a change in orientation within lattice cells which allows for an adaptation of directional dependent elastic properties of TPMS lattice structures during design and optimization. To ultimately align the anisotropy of microstructures to stress direction, it is critical to release the rotational freedom of the unit lattice cell parameterization, in a manner similar to that done by Bendsoe and Kikuchi [27] in their homogenization method. The distribution of lattice orientation in the design domain would allow for an adaptation of each unit cell anisotropy to the local stress direction, rather than controlling the anisotropy by assembly two different base units to form a new representative unit as in [28].

However, there are some limitations on the spatial variant lattice construction. The orientation can infill volume fraction distribution field should be continuous, the significant local distortion will result if the difference between neighboring cell angles is greater than  $45^\circ$ . For large angle difference, the standard triply symmetric TPMS structure will no longer exist in the distorted unit cell as the adaptation of orientation difference. In this case, the neck area is elongated to offset the lattice distortion. Furthermore, the construction algorithm will lead to the lattice shift outside of the unit cell boundary to keep the required smooth transition due to the varying grating phase.

The relationship between the variant volume fraction of the TPMS and iso-surface parameter  $t$  is not a linear one. Typically, the relative density of the unit lattice is controlled by changing the value of  $t$  to change the enclosed volume of the 3D surface or offsetting  $t$  to produce surface-based on lattice. Due to the introduction of infill fraction that is caused by the threshold method in the current algorithm, the relationship between  $t$  and volume fraction no longer exists. In this case, the relative density can be extracted from the summation of binary pixel by comparing pixel values with the threshold value. A more accurate volume fraction is obtained by recalculating the summation of the volumes of tetrahedron after meshing the enclosed patch surface.

Compared to the laminate TPMS lattice structure produced by recursive skew transformation, the current lattice structure shifts out of the unit cell after spatial transformation. Due to the continuous orientation accumulation in one direction which is like the wave accumulation in propagation, the rotation of cells in Y direction leads to the skew shift in the X direction. If the orientation angle difference is small, this defect will disappear. However, the morphological variation generated by the spatially varying algorithm keeps a smooth transition while varying the lamina orientation, but the hybrid design with skew transformation does not. Besides, if the relative volume fraction is lower, the connectivity between each layer is destroyed as shown in Fig. 4 (a).

Since the spatial variant lattice needs to decompose to the planar grating vector in order to incorporate the varying orientation and solve for the grating phase, the presented research is limited to a primitive network or scaffold based TPMS lattice structure and is not applicable to surface-based lattices. There are two approaches to extend the current algorithm to other types of scaffold-based lattices, such as Gyroid, IWP and Diamond. From the generalized method, the

orientation can be introduced to the truncated and decomposed Fourier terms to construct the mapping equation, which is not very computation efficient. The more elegant approach takes less computation resources, since the unit TPMS lattice can be generated by the basic reciprocal vector as mentioned before [18], where the number of reciprocal vectors is far less than the truncated Fourier terms. The rotation matrices can be applied on the reciprocal vectors directly to construct the mapping equation and later solved by the finite difference method. With the solution of mapping function, the spatially varying TPMS lattices can be reconstructed by the generalized exponential expression.

In addition, the present algorithm cannot distribute the TPMS lattice type simultaneously according to user-defined boundaries. Hence, two different methods were proposed to design heterogeneous TPMS lattice structures with varying orientation distribution. Unfortunately, the introduction of varying orientation within the lattices may lead to uncertain defects such as the sharp corners or unconnected ligaments when it comes to the heterogenous lattice structures.

The transformed lattice under varying orientation needs to be combined with the cubic symmetric TPMS lattice to produce the heterogenous lattice structures, where the defects between different types of lattices is unavoidable. The IWP type lattice is more compatible with Primitive type (similar with Body-centered Cubic) than Gyroid shown as Fig. 5 and Fig. 6, due to the BCC lattice (Primitive type) with varying orientation being closer to the geometric configuration of Face-Centered Cubic (FCC). In addition, the transition area produced by the distance field function shows a better geometry connectivity, however, it is necessary to evaluate its construction quality by finite element analysis in the future research.

## **5. Conclusion**

In summary, a novel method is proposed to design spatially varying TPMS lattice structures with varying infill volume fraction and varying spatial orientation. An iterative central finite difference method was applied to solve the partial differential equation governing the relationship between varying orientation and position. The current method can be utilized to optimized directional dependent TPMS lattice structure to align principal stress with the lattice geometry configuration within the design domain. In addition, the heterogeneous lattice with varying orientation is explored by GRBF and the distance field function where the later one is shown to produce better structure transitions between different lattice types. By introducing the lattice varying volume fraction, unit cell variant orientation and lattice type distribution, more freedom is offered to the design domain of TPMS lattice structures.

## Reference

- [1] Alabort, Enrique, Daniel Barba, and Roger C. Reed. "Design of metallic bone by additive manufacturing." *Scripta Materialia* 164 (2019): 110-114.
- [2] Arabnejad, Sajad, et al. "Fully porous 3D printed titanium femoral stem to reduce stress-shielding following total hip arthroplasty." *Journal of Orthopaedic Research* 35.8 (2017): 1774-1783.
- [3] Pouya, Caroline, et al. "Characterization of a mechanically tunable gyroid photonic crystal inspired by the butterfly *parides sesostris*." *Advanced Optical Materials* 4.1 (2016): 99-105.
- [4] Torres-Sanchez, Carmen, et al. "Comparison of Selective Laser Melted Commercially Pure Titanium Sheet-Based Triply Periodic Minimal Surfaces and Trabecular-Like Strut-Based Scaffolds for Tissue Engineering." *Advanced Engineering Materials* 24.1 (2022): 2100527.
- [5] Dang, Bao-Loi, et al. "Mechanical and hydrodynamic characteristics of emerged porous Gyroid breakwaters based on triply periodic minimal surfaces." *Ocean Engineering* 254 (2022): 111392.
- [6] Feng, Jiawei, et al. "Triply periodic minimal surface (TPMS) porous structures: From multi-scale design, precise additive manufacturing to multidisciplinary applications." *International Journal of Extreme Manufacturing* 4.2 (2022): 022001.
- [7] Yoo DJ. New paradigms in internal architecture design and freeform fabrication of tissue engineering porous scaffold *Med Eng Phys*, 34 (2012), pp. 762-776
- [8] Leong, K., Chua, s.C., Sudarmadji, N., Yeong, W., 2008. Engineering functionally graded tissue engineering scaffolds. *J. Mech. Behav. Biomed. Mater.* 1, 140–152
- [9] Yang, N., Quan, Z., Zhang, D., Tian, Y., 2014. Multi-morphology transition hybridization CAD design of minimal surface porous structures for use in tissue engineering. *Comput. Aided Des.* 56, 11–21
- [10] Yoo, Dongjin. "Heterogeneous minimal surface porous scaffold design using the distance field and radial basis functions." *Medical engineering & physics* 34.5 (2012): 625-639.
- [11] Afshar, M., et al. "Additive manufacturing and mechanical characterization of graded porosity scaffolds designed based on triply periodic minimal surface architectures." *Journal of the mechanical behavior of biomedical materials* 62 (2016): 481-494.
- [12] Cheikho, K., Cédric Laurent, and J. F. Ganghoffer. "An advanced method to design graded cylindrical scaffolds with versatile effective cross-sectional mechanical properties." *Journal of the mechanical behavior of biomedical materials* 125 (2022): 104887.
- [13] Ma, Songhua, et al. "Biological and mechanical property analysis for designed heterogeneous porous scaffolds based on the refined TPMS." *Journal of the Mechanical Behavior of Biomedical Materials* 107 (2020): 103727.
- [14] *Philosophical Transactions: Mathematical, Physical and Engineering Sciences*, Sep. 16, 1996, Vol. 354, No. 1715, Curved Surfaces in Chemical Structure (Sep. 16, 1996), pp. 2077-2104
- [15] Schwarz, H. 1890 *Gesammelte Mathematische Ahhandlungen*. Berlin: Springer
- [16] Campbell, M. T. H. R. G. D. M., et al. "Fabrication of photonic crystals for the visible spectrum by holographic lithography." *Nature* 404.6773 (2000): 53-56.

- [17] R. C. Rumpf and J. Pazos, "Synthesis of spatially variant lattices," *Opt. Express*, vol. 20, no. 14, p. 15263, Jun. 2012.
- [18] Moon, Jun Hyuk, Jamie Ford, and Shu Yang. "Fabricating three-dimensional polymeric photonic structures by multi-beam interference lithography." *Polymers for Advanced Technologies* 17.2 (2006): 83-93.
- [19] R. C. Rumpf, "Lecture #18a--Synthesis of Spatially-Variant Planar Gratings." El Paso, p. 6, 2018.
- [20] Digaum, J. L., "Fabrication and characterization of spatially-variant self-collimating photonic crystals," University of Central Florida Dissertation, (2016).
- [21] Berry, Eric A., and Raymond C. Rumpf. "Generating spatially-variant metamaterial lattices designed from spatial transforms." *Progress In Electromagnetics Research M* 92 (2020): 103-113.
- [22] Rastegarzadeh, Sina, Jun Wang, and Jida Huang. "Two-Scale Topology Optimization with Isotropic and Orthotropic Microstructures." *Designs* 6.5 (2022): 73.
- [23] Ren, Fangxi, et al. "Transition boundaries and stiffness optimal design for multi-TPMS lattices." *Materials & Design* 210 (2021): 110062.
- [24] Fasshauer, Gregory E. *Meshfree approximation methods with MATLAB*. Vol. 6. World Scientific, 2007.
- [25] Yang, Nan, et al. "Building implicit-surface-based composite porous architectures." *Composite Structures* 173 (2017): 35-43.
- [26] Yang, Nan, et al. "Anisotropy and deformation of triply periodic minimal surface based lattices with skew transformation." *Materials & Design* (2023): 111595.
- [27] Bendsoe MP, Kikuchi N (1988) Generating optimal topologies in structural design using a homogenization method. *Computer Methods in Applied Mechanics and Engineering* 71(2):197–224, DOI 10.1016/0045-7825(88)90086-2
- [28] Xu, Shanqing, et al. "Design of lattice structures with controlled anisotropy." *Materials & Design* 93 (2016): 443-447.